Numerical and Experimental Investigations of Fluidic Thrust Vectoring

Numerical and Experimental Investigations of Fluidic Thrust Vectoring

特　　　集

Numerical and Experimental Investigations of Fluidic Thrust Vectoring

Li LI*, Mitsutomo HIROTA** and Tsutomu SAITO**

Fluidic thrust vectoring (FTV), an ability of air vehicles to manipulate the nozzle flow deflect their longitudinal axis, can satisfy the modern aircraft requirements dramatically. Numerical and experimental studies of FTV are performed with a nozzle pressure ratio (NPR) of 4–10, a secondary pressure ratio (SPR) of 1, 2 or 3, and two different secondary jet locations. Numerical simulations of the nozzle flow are done with solving the Navier-Stokes equations, and the input parameters are set to match the experimental conditions. The thrust pitching moment and the thrust pitching angle are determined to evaluate the FTV performance.

Keywords : Fluid thrust vectoring, Converging-diverging nozzle, CFD, Secondary jet

1　INTRODUCTION

The desirable design goal of modern jet aircraft is to increase the maneuverability, agility, and survivability. The Fluidic thrust vectoring (FTV) is a significant technology for high-performance air vehicles. The technology can improve aircraft performance by manipulating the nozzle flow to deflect from its axial direction. FTV involves a directional alteration of the main exhaust gas flow by a secondary jet in the nozzle diverging part. Potentially, FTV nozzles provide effective flow deflection with less weight, low noise, simplicity, low maintenance costs, etc. [1][2].

The objectives of this study are to investigate the effect of a secondary jet on the primary flow in a converging-diverging nozzle, to discuss the effect of

* Department of Mechanical Engineering, Dalian Jiaotong University, 794 Huanghe Road, Shaheko District, Dalian 116028, CHINA
** Department of Aerospace Engineering, Muroran Institute of Technology, 27-1 mizumoto-cho, Muroran, Hokkaido 050-8585, JAPAN

FTV parameters, and to evaluate the FTV performance.

2　EXPERIMENTAL SETUP

The experimental setup is shown in Fig. 1. The inlet of the nozzle is open to the atmosphere, whereas the outlet is connected to a vacuum tank. The back pressure of the nozzle is kept practically constant at 0.1atm during a typical test time of 5–10 s [3][4]. The Schlieren system and the pressure gauges are used to obtain the experimental data.
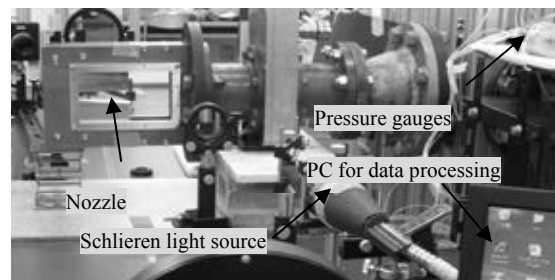

Fig. 1 Experimental setup

The nozzle is designed to rotate around the rotation shaft to adjust the exit spacing while keeping the throat

spacing constant. The area ratio of the nozzle exit to the throat area is 1.69 with flow Mach number of 2. The secondary jet injection slot on the upper nozzle wall has a width of 1 mm. Figure 2 shows the dimensions of nozzle with secondary jet injection slot adjusted to the flow Mach number of 2.
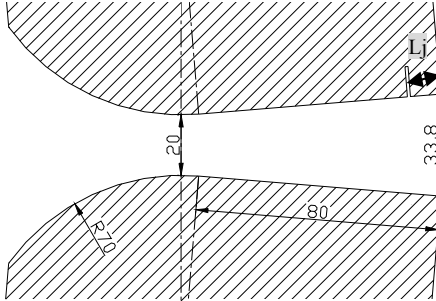

Fig. 2 Dimensions of nozzle at Mach number of 2.

3   NUMERICAL METHOD

The Reynolds number of the flow at the nozzle exit corresponds to the transition zone from laminar to turbulent flow. The flow at the inlet is accelerated from the stationary atmosphere and the transition is suppressed till relatively high Reynolds number. This is visually confirmed with Schlieren images. Therefore, in this study, the flow is assumed to be laminar. The Navier-Stokes equations are solved numerically. The numerical fluxes are evaluated with the HLLC Riemann solution, and the numerical simulations were carried out with the WAF method [5].

4   EVALUATION OF FTV PERFORMANCE

The FTV performance is evaluated by thrust pitching angle δ [6][7].

$$\delta = \tan^{-1}(F_N / F_A), \tag{1}$$

where F_A and F_N are the x and y components of momentum.

The thrust pitching moment M of the nozzle is expressed by

$$M = \sum (F_w \cdot l), \tag{2}$$

where F_w is the working pressure on the nozzle walls and l is the length from the working point to the pivot point.

5   RESULRTS AND DISCUSSIONS

The conditions in experiments and numerical simulations range are nozzle pressure ratio (NPR) from 4 to 10, the secondary pressure ratio (SPR) from 1, 2 to 3, with the spacing between the secondary jet injection slot and the nozzle exit Lj = 5 mm and Lj = 10 mm.

The effects of FTV parameters such as NPR, SPR, Lj, and angular injection angle β on the FTV performance are discussed.

5.1 Effect of NPR

Numerically obtained Mach number distribution with NPR = 9 is shown in Fig. 3. The Mach number in the nozzle diverging part increases from 1 to 2. The Mach number of two-dimensional (2-D) numerical results at the nozzle throat is not the same as the one-dimensional (1-D) theory. For the 1D theory, the Mach line is a straight line at the throat with Mach number of 1 while for the 2-D numerical method, the Mach line is an arch. In addition, the Mach number of 2-D at the nozzle exit is close to the designed value of 2. It is seen that the Mach number reaches 3 at a small regions downstream of the nozzle exit.
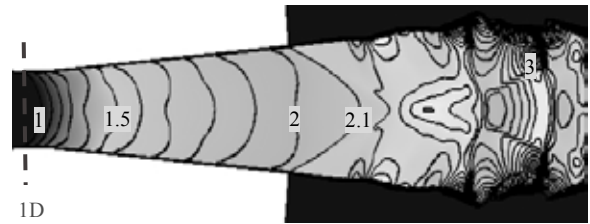

Fig. 3 Mach number distribution in the nozzle diverging part with NPR = 9.

5.2 Effect of SPR

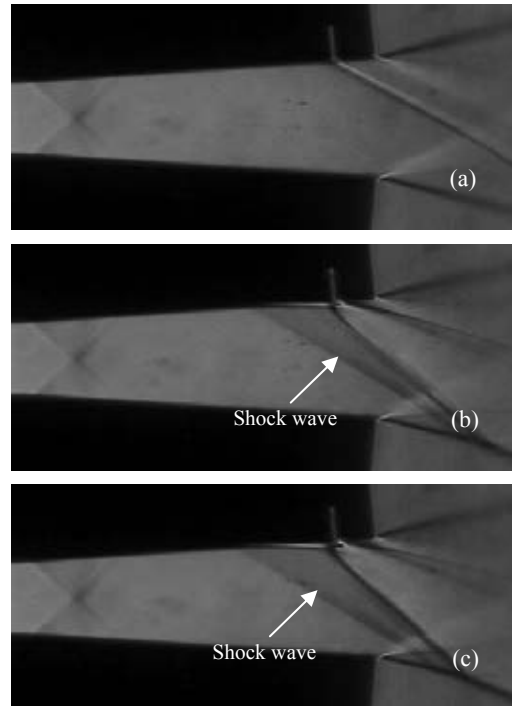Figure 4 shows the Schlieren images for Lj = 10 mm with NPR = 9 and SPR = 1, 2 or 3.

Fig. 4 Schlieren images for Lj = 10 mm with NPR = 9 and (a) SPR = 1 or (b) SPR = 2 (c) SPR = 3.

With SPR = 1, the secondary jet is visible as a bright line starting from the secondary jet slot, as seen in Fig. 4(a). As SPR increases, the jet continue to spread, and the separation domain near the wall upstream the jet

also becomes larger as shown in Fig. 4(b) and Fig. 4(c). It is found that the basic flow patterns are the same with Lj = 5 mm.

In order to investigate the effect of SPR quantitatively, Table 1 shows the thrust pitching moment with NPR = 9 at different SPR and Lj. It is observed that the moment of Lj = 10 mm is smaller than that of Lj = 5mm. The moment increases from SPR = 1 to SPR = 2 and then decreases at the SPR = 3 possibly due to shock reflection on the other wall.

Table 1 Thrust pitching moment at different SPR and Lj.

M [N·m]	SPR = 1	SPR = 2	SPR = 3
Lj =5 mm	11.8	14.9	13.8
Lj = 10 mm	9.5	10.6	9.6

Table 2 Thrust pitching angle at different SPR and Lj.

δ [deg]	SPR = 1	SPR = 2	SPR = 3
Lj =5 mm	5.0	7.4	8.6
Lj = 10 mm	4.4	6.3	7.7

Table 2 shows the thrust pitching angle with NPR = 9 at different SPR and Lj. It is observed that deflection angle of Lj = 10 mm is smaller than that of Lj = 5 mm. The angle increases as the SPR increases. The change tendency of deflection angle is not the same as the moment for the possible tiny reflection has not effect on the deflection angle.
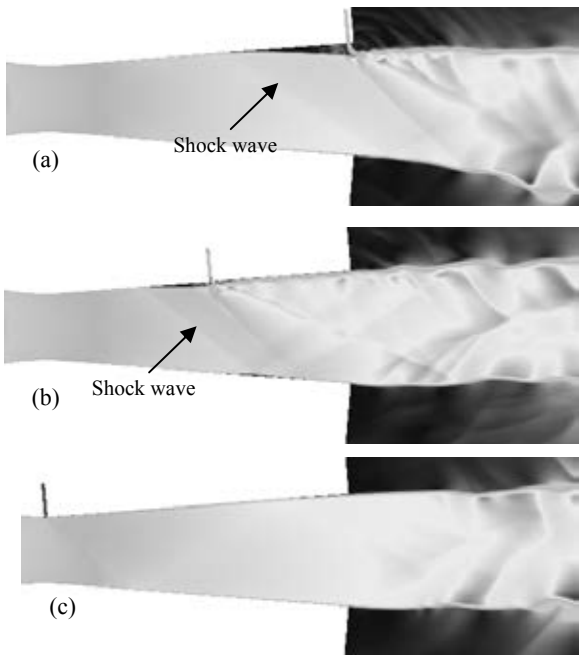
5.3 Effect of Lj

(a)
Shock wave

(b)
Shock wave

(c)

Fig. 5 Mach number distribution with NPR = 9 and SPR=1 and (a) Lj = 2 mm or (b) Lj = 40 mm or (c) Lj = 80 mm.

Figure 5 shows the flow Mach number distribution with NPR = 9 and SPR = 1 for different values of and Lj = 2, 40 and 80 mm. As the location of the secondary jet injection is near to the exit, the deflection of flow is large, as shown in Fig. 5(a). As the location of the secondary jet injection is moved to the throat, the induced oblique shock wave reflects at the opposite nozzle wall even for SPR = 1, as shown in Fig. 5(b). In the case of secondary jet injection being placed at the nozzle throat, there are no obvious interaction between the secondary injection and the primary flow, as shown in Fig. 5(c).

5.4 Effect of β

The effect of secondary jet injection angle is investigated by defining the angular injection angle β as in Fig. 6.
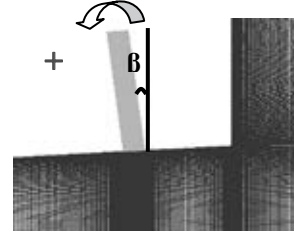

Fig. 6 Illustration of secondary angular injection.

Figure 7 shows the thrust pitching moment at different β with NPR = 9. When the β is positive, the moment decreases and the moment for SPR = 2 is larger than SPR = 1 except β = 70°. Whereas when the β is negative, the change tendency of the moment with SPR = 1 is different from that with SPR = 2. The biggest moment of SPR = 1 occurs with β = –45°. The negative of the moment at β = 70° is caused by the reflection on the nozzle wall.
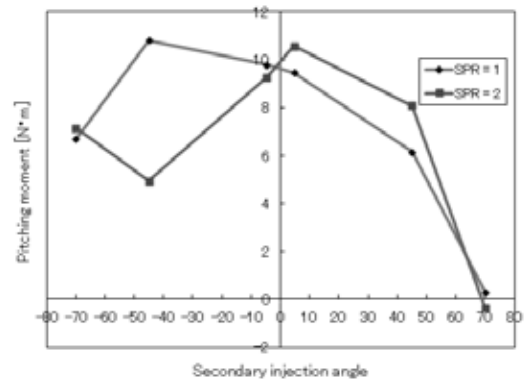

Fig. 7 Thrust pitching moment at different β with NPR=9.

Figure 8 shows the pitching angle at different β with NPR = 9. It is observed the angle change tendency is the same as that of the pitching moment. When β is positive, the largest angle with SPR = 1 happens with the largest moment. Whereas for SPR = 2, the largest
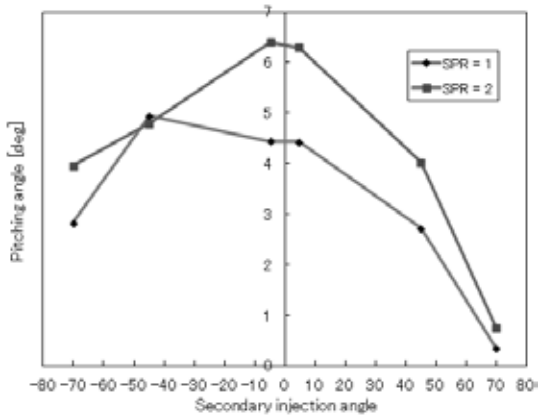
angle happens with β near 0°.

Fig. 8 Thrust pitch angle at different β with NPR = 9.

5   CONCLUSIONS

In order to study the details of the FTV performance, the experimental model with a smaller secondary jet slot is constructed. The effects of FTV parameters, such as NPR, SPR, Lj and angular injection angle β are discussed.

The performance of FTV is evaluated by thrust pitching moment and thrust pitching angle. The thrust pitching moment is positive as expected induced by an oblique shock wave.

The larger SPR causes the decreased moment due to the possible tiny reflection on the opposite nozzle wall, but it has no effect on the deflection angle.

As the secondary jet slot moves to the nozzle throat, the effect of the secondary jet on the pitching moment and the deflection angle becomes weak.

For different secondary angular injection β, the positive and negative cases should be separated to discuss. For positive β, the moment and deflection angle decreases as the β increases, and the moment of higher SPR is larger. For negative β, the change tendency of the moment and the deflection angle is different with different SPR.

REFERENCE

(1) Rickey J. Shyne, A Survey of Challenges in Aerodynamic Exhaust Nozzle Technology for Aerospace Propulsion Applications, NASA/TM-2002-211977.

(2) A. J. Neely , F. N. Gesto and J. Young, Performance Studies of Shock Vector Control Fluidic Thrust Vectoring, AIAA-2007-5086, 43rd AIAA/ ASME/ SAE/ ASEE Joint Propulsion Conference & Exhibit, Cincinnati, OH, 2007.

(3) Li Li, Tsutomu Saito, Numerical and Experimental Investigations of Fluidic Thrust Vectoring Mechanism, International Journal of Aerospace Innovations, UK, 2011.

(4) L. Li, M. Hirota, and T. Saito ，Numerical and Experimental Studies of Fluidic Thrust Vectoring, 28th International Symposium on Shock Waves, UK, 2011.

(5) E. F. Toro, V. A. Titarev, Solution of the Generalized Riemann Problem for Advection–Reaction equations, Proceedings of the Royal Society, 2002.

(6) Mark S. Mason, William J.Crowther, Fluidic Thrust Vectoring of Low Observable Aircraft, CEAS Aerospace Aerodynamic Research Conference, 2002

(7) K. A. Waithe and K. A. Deere, Experimental and Computational Investigation of Multiple Injection Ports in a Convergent-divergent Nozzle for Fluidic Thrust Vectoring, the 21st AIAA Applied Aerodynamics Conference, AIAA-2003-3802.